Ruthenium(II/III)–bipyridine complexes with four-membered sulphur donor co-ligands: synthesis, metal valence preference, spectroscopic and electron-transfer properties

Shilpa S. Kulkarni, Bidyut Kumar Santra, Pradip Munshi and
Goutam Kumar Lahiri*

Department of Chemistry, Indian Institute of Technology, Powai, Bombay, Mumbai 400076, India

Abstract—A group of stable ruthenium(II) and (III) mixed-ligand tris-chelated complexes of the type $[Ru^{n+}(bpy)(L)_2]^{z+}$ (**1**–**8**, $n=2$, $Z=0$; **9**, $n=3$, $Z=1$) have been synthesized and characterized (bpy = 2,2′-bipyridine; L = anionic form of the ligands, ROC(S)SK, (R = Me, Et, ^{n}Pr, ^{i}Pr, ^{n}Bu, ^{i}Bu, –CH_2–Ph) or $(EtO)_2P(S)SNH_4$ or $(Et)_2NC(S)SNa$). The complexes **1**–**8** are diamagnetic and electrically neutral and the complex **9** is one-electron paramagnetic and behaves as 1:1 electrolyte in acetonitrile solvent. The complexes **1**–**8** and **9** display two MLCT transitions near 530, 370 nm and 663, 438 nm respectively. Intra-ligand bipyridine based π–π^* transition is observed near 300 nm. The complexes **1**–**8** exhibit room-temperature emission from the highest energy MLCT band (~370 nm). At room temperature the lifetime of the excited states for the complexes **2** and **8** are found to be 90 and 95 ns respectively. In acetonitrile solution the complexes **1**–**9** show a reversible ruthenium(III)–ruthenium(II) couple in the range $-0.08 \rightarrow 0.40$ V and irreversible ruthenium(III)–ruthenium(IV) oxidation in the range 1.19–1.45 V vs Ag/AgCl. One reversible bipyridine reduction is observed for each complex in the range $-1.70 \rightarrow -1.85$ V vs Ag/AgCl. The presence of trivalent ruthenium in the oxidized solution for one complex **1** is evidenced by the axial EPR spectrum at 77 K. The isolated trivalent complex **9** also exhibits an axial EPR spectrum at 77 K. The EPR spectra of the trivalent ruthenium complexes (**1**$^+$ and **9**) have been analyzed to furnish values of distortion parameters ($\Delta(cm^{-1}) \rightarrow$ **1**$^+$, 3689; **9**, 3699) and energies of the two expected ligand field transitions ($\nu_1(cm^{-1}) \rightarrow$ **1**$^+$, 3489; **9**, 3497 and $\nu_2(cm^{-1}) \rightarrow$ **1**$^+$, 4339; **9**, 4348) within the t_2 shell. One of the ligand field transitions has been experimentally observed at 4673 cm^{-1} for complex **9** and which close to the computed ν_2 value (4348 cm^{-1}).

INTRODUCTION

Since the discovery of important photo-redox properties of ruthenium–bipyridine complexes, there has been continuous research activity in this area [1–12]. Here the main thrust has been primarily focused on the development of newer ruthenium–bipyridine systems with the perspective of interesting physico-chemical properties. Basic strategies behind all these activities are either to incorporate selective groups within the bipyridine moiety itself or use other types of donor sites along with the ruthenium--bipyridine core to generate mixed-ligand mononuclear or polynuclear complexes to modulate the photo-redox activities of this class of complexes [13–28]. The present work originates from our interest in preparing new mixed-ligand ruthenium–bipyridine complexes of type $[Ru(bpy)(L)_2]$, where L is a sulphur donor ligand which can form a four-membered chelate ring on coordination and in studying the effect of sterically hindered S,S donor ligands L on the redox and spectroscopic properties of the Ru–bpy core. As a part of our program here we have chosen dithiocarbonate, $ROC(S)S^-$; dithiophosphate, $(RO)_2P(S)S^-$ and dithiocarbamate $(R)_2NC(S)S^-$ as ligand L. Herein we report the synthesis of three classes of complexes having RuN_2S_4 chromophore, their spectroscopic and electrochemical properties, spectroelectrochemical correlation and preliminary photophysical aspects. To the best of our knowledge this work demonstrates the first example of $[Ru(bpy)(L)_2]$ complexes where L is a sterically hindered four-membered sulphur donor ligand.

RESULTS AND DISCUSSION

Synthesis

Three types of S,S donor ligands, potassium salt of dithiocarbonate ($KL^{1\text{–}7}$), ammonium salt of dithiophosphate (NH_4L^8) and sodium salt of dithiocarbamate (NaL^9) are used for the present study.

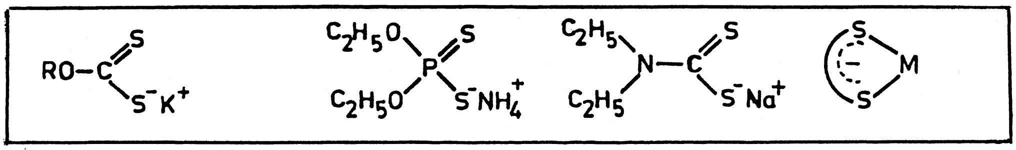

The anionic form of the ligands (L^-) bind to the metal ion as bidentate S,S coordinators forming a four-membered chelate ring (ML).

The complexes, $[Ru^{II}(bpy)(L^{1\text{–}8})_2]$ (**1**–**8**) and $[Ru^{III}(bpy)(L^9)_2]^+$ (**9**) (bpy = 2,2′-bipyridine) have been synthesized from $[Ru(bpy)Cl_3]$ following the general dechlorination route shown in Scheme 1.

The reactions of potassium salt of dithiocarbonate ligands ($KL^{1\text{–}7}$) with the starting complex $Ru(bpy)Cl_3$ spontaneously result in red colored complexes **1**–**7** at room temperature, whereas the reaction of ammonium salt of dithiophosphate NH_4L^8 with the $Ru(bpy)Cl_3$ requires slight heating to yield the violet colored complex **8**. The crude products **1**–**8** were purified by column chromatography using silica gel column.

The reaction of sodium salt of diethyl dithiocarbamate with the $Ru(bpy)Cl_3$ under stirring condition at room temperature yields green colored cationic complex **9**. The cationic complex **9** has been isolated as perchlorate salt, $[Ru^{III}(bpy)(L^9)_2]ClO_4$.

Although dithiocarbonate ($L^{1\text{–}7}$) and dithiophosphate (L^8) ligands stabilize the ruthenium ion in the complexes **1**–**8** in bivalent Ru(II) state, the corresponding dithiocarbamate complex **9** stabilizes the trivalent Ru(III) state. The chemically and electrochemically generated trivalent Ru(III) congeners of complexes **1**–**8** and bivalent Ru(II) congener of complex **9** are unstable at room temperature (see later). The bipyridine ligand is known to stabilize the bivalent ruthenium due to its strong π-acidic nature [13–28]. Since all the three types of complexes (**1**–**7**, **8** and **9**) consist of one bipyridine ligand common, the observed metal oxidation state preference in the complexes (**1**–**9**) is therefore naturally originated from the inducted dithio ligands ($L^{1\text{–}9}$).

The stabilization of Ru(III) state in the case of dithiocarbamate complex (**9**) is not clearly under-

$$Ru(bpy)Cl_3 + KL^{1\text{–}7} \xrightarrow{(i)} \underset{\mathbf{1\text{–}7}}{[Ru^{II}(bpy)(L^{1\text{–}7})_2]}$$

$$Ru(bpy)Cl_3 + NH_4L^8 \xrightarrow{(ii)} \underset{\mathbf{8}}{[Ru^{II}(bpy)(L^8)_2]}$$

$$Ru(bpy)Cl_3 + NaL^9 \xrightarrow{(iii)} \underset{\mathbf{9}}{[Ru^{III}(bpy)(L^9)_2]^+}$$

Ligand		Complex
L^1	→	**1**
L^2	→	**2**
L^3	→	**3**
L^4	→	**4**
L^5	→	**5**
L^6	→	**6**
L^7	→	**7**
L^8	→	**8**
L^9	→	**9**

Scheme 1. (i) MeOH, stirring, (ii) MeOH, heat and (iii) MeOH, stirring.

stood, however, the inherent electronegativity difference between the N atom of L^9 and oxygen atom of $L^{1\text{–}7}$ and the π-acceptor nature of the phosphorus of L^8 might be responsible for the above valence state preference in the complexes **1**–**9**.

The microanalytical data of the complexes are shown in Table 1. The results are in good agreement with the calculated values thus confirming the composition of the mixed-ligand tris-chelates [Ru(bpy)($L^{1\text{–}8}$)$_2$] (**1**–**8**)] and [Ru(bpy)(L^9)$_2$]ClO_4 (**9**). In acetonitrile solution the complexes **1**–**8** do not show any conductivity whereas the complex **9** exhibits 1:1 conductivity (Λ_M, 150 Ω^{-1} cm^2 M^{-1}). Solid state magnetic moment measurements at 298 K indicate that the complexes **1**–**8** are essentially diamagnetic ($t_{2g}{}^6$, idealized $S = 0$) and complex **9** is one-electron paramagnetic ($\mu_{\text{eff}} = 1.91\ \mu\beta$) as expected for the 3+ state of ruthenium (low-spin d^5, $S = 1/2$).

Spectral study

IR spectra FTIR spectra of the complexes (**1**–**9**) were recorded as KBr discs. Direct comparisons of the IR spectra of **1**–**9** with that of the starting complex [Ru(bpy)Cl_3] indicate that the $\nu_{\text{Ru–Cl}}$ vibrations near 330 cm^{-1} [29] are absent in the former complexes and new vibrations due to the coordinated ligands L are systematically present in the complexes (**1**–**9**). A very strong and broad vibration at 1098 cm^{-1} and a strong and sharp band at 624 cm^{-1} are observed for the complex **9** due to the presence of ionic perchlorate.

^{1}H *NMR spectra* In $CDCl_3$ solvent, all the complexes (**1**–**8**) display well resolved ^{1}H NMR spectra. The spectral data are listed in Table 2 and two representative spectra are shown in Fig. 1. The assignment of the individual proton resonances are made on the basis of their relative intensity and spin–spin structure [30]. All the complexes (**1**–**8**) should have plane of symmetry and this makes each half of the molecule equivalent. In view of the imposed symmetry around the ruthenium center aromatic region of the spectra of complexes (**1**–**6** and **8**) displaying systematically four signals having equal intensities (two doublets and two triplets) (Fig. 1) correspond to one pyridine ring of bipyridine ligand. In the case of complex **7** aromatic region of the spectrum shows additional peaks due to phenyl ring attached to the dithiocarbonate ligand (L^7) (Table 2). The phenyl ring protons are not resolved properly and all the five protons have appeared as one complex signal centered at 7.36 ppm (Table 2), which precluded unequivocal assignment of the signals as doublets or triplets. However, the presence of five phenyl ring protons is clearly observable from the relative intensity of the peaks. Depending on the nature of L aliphatic region of the spectra display distinct signals for O–CH_3, O–CH_2, O–CH, –CH, –CH_2 and –CH_3 protons correspond to one ligand (L) as imposed symmetry makes the two

Table 1. Microanalytical, electronic absorption and emission data

Compound	Elemental analysis (%)[a]			Electronic spectral data[b] $\lambda_{\max}$ (nm) (ε[c], M^{-1} cm^{-1})	Emission data[b]	
	C	H	N		$\lambda_{\max}$ (nm)	$\lambda_{\max}$ (nm)
1	35.55 (35.66)	2.89 (2.97)	5.82 (5.94)	531(4480), 401(6750)[d], 365(7660), 299(13870)	365	429
2	38.56 (38.47)	3.51 (3.60)	5.75 (5.61)	537(4500), 401(5750)[d], 370(6720), 298(12300),	370	423
3	40.84 (40.97)	4.13 (4.17)	5.25 (5.31)	538(3860), 399(5500)[d], 374(6000), 298(11820)	374	420
4	40.82 (40.97)	4.22 (4.17)	5.46 (5.31)	540(6280), 403(8000)[d], 374(9420), 299(13620)	374	430
5	43.37 (43.23)	4.75 (4.68)	5.16 (5.04)	537(4810), 400(6750)[d], 370(8050), 299(13400)	370	421
6	43.32 (43.23)	4.61 (4.68)	4.92 (5.04)	539(6760), 403(8000)[d], 373(9280), 299(13400)	373	424
7	50.19 (50.07)	3.65 (3.53)	4.33 (4.49)	524(3400), 407(5600)[d], 365(6250), 299(12810)	365	433
8	34.55 (34.44)	4.52 (4.46)	4.37 (4.46)	528(3080), 380(5160), 299(13010)	380	429
9	36.82 (36.77)	4.17 (4.29)	8.71 (8.58)	663(1610), 438(3150), 340(8000)[d], 301(13950)	–	–

[a] Calculated values are in parentheses.

[b] In acetonitrile solution.

[c] Extinction coefficient.

[d] Shoulder.

Table 2. ^{1}H NMR spectral data in $CDCl_3$

Compound	δ (J/Hz)[a]											
	6H	3H	4H	5H	$-OCH_3$	$-OCH_2$	–OCH	–CH	$-CH_2(1)$	$-CH_2(2)$	$-CH_3$	–ph
1	9.45 (7.20)[b]	8.04 (9.30)[b]	7.67 (7.5)[c] (7.5)	7.35 (6.5)[c] (6.5)	4.12[d]	–	–	–	–	–	–	–
2	9.46 (7.69)[b]	8.03 (9.73)[b]	7.65 (9.73)[c] (8.76)	7.34 (8.11)[c] (8.11)	–	4.60 (7.08)[e] (7.08) (7.08)	–	–	–	–	1.44 (7.32)[c] (7.32)	–
3	9.46 (7.67)[b]	8.02 (7.06)[b]	7.64 (7.06)[c] (7.06)	7.33 (7.06)[c] (7.06)	–	4.50 (7.10)[c] (7.10)	–	–	1.84[f]	–	1.01 (7.06)[c] (7.06)	–
4	9.46 (7.69)[b]	8.01 (9.73)[b]	7.64 (8.92)[c] (9.72)	7.32 (8.11)[c] (8.91)	–	–	5.56[f]				1.43 (6.00)[b] 1.37 (6.00)[b]	–
5	9.44 (7.69)[b]	8.01 (7.94)[b]	7.62 (7.94)[c] (7.94)	7.31 (6.17)[c] (7.02)	–	4.53 (7.50)[c] (6.50)	–	–	1.78[f]	1.43[f]	0.92 (8.18)[c] (8.18)	–
6	9.45 (7.69)[b]	8.00 (7.10)[b]	7.63 (7.71)[c] (7.71)	7.33 (6.85)[c] (7.71)	–	4.30 (7.69)[b]	–	2.12[f]			1.02 (7.06)[b] 0.95 (6.17)[b]	–
7	9.40 (7.90)[b]	8.01 (8.10)[b]	7.65 (7.92)[c] (7.87)	7.45 (8.10)[c] (7.65)		5.59 (9.37)[e] (9.37) (9.37)						7.36[g]
8	9.94 (8.50)[b]	7.96 (6.80)[b]	7.61 (6.85)[c] (7.50)	7.35 (8.20)[c] (7.60)	–	4.22 (7.60)[e] (3.91) (8.30)[e]	–	–	–	–	1.34 (6.43)[c] (6.48) 1.23 (6.72)[c] (6.72)	–

[a] Tetramethyl silane is the internal standard.
[b] Doublet.
[c] Triplet.
[d] Singlet.
[e] Quartet.
[f] Multiplet, center value is given.
[g] Overlapping phenyl protons, center value is given.

ligands (L) equivalent in the complexes. In fact the upfield region of the spectra displaying excellent distribution pattern of the aliphatic proton signals (Table 2). In all cases experimentally observed relative ratio of aromatic protons to aliphatic protons matches very well with the calculated values.

Electronic spectra The solution electronic spectra of the complexes (**1**–**9**) were recorded in acetonitrile solvent in the UV–visible region (200–900 nm). The spectral data are listed in Table 1 and the representative spectra are shown in Fig. 2. The absorption spectra of all the complexes **1**–**8** are similar and showing one intense transition in the UV region and two moderately intense transitions in the visible region near 530 and 370 nm. The 370 nm band is associated with a shoulder at the lower energy part near 400 nm (Table 1). The lowest energy bands near 530 and 400 nm can be attributed to $d\pi(Ru) \rightarrow \pi^*(bpy)$ (symmetric) and $d\pi(Ru) \rightarrow \pi^*(bpy)$ (antisymmetric) MLCT transitions [31–36]. The next higher energy band near 370 nm may be due to $d\pi(Ru) \rightarrow L$(MLCT) transition. The absorption at 300 nm is assigned to π–π^* ligand centered (bpy) transition. It may be noted that the lowest energy MLCT transition of $[Ru(bpy)_3]^{2+}$ appears at 452 nm [37] gets substantially shifted to a lower energy (~ 530 nm) on substituting

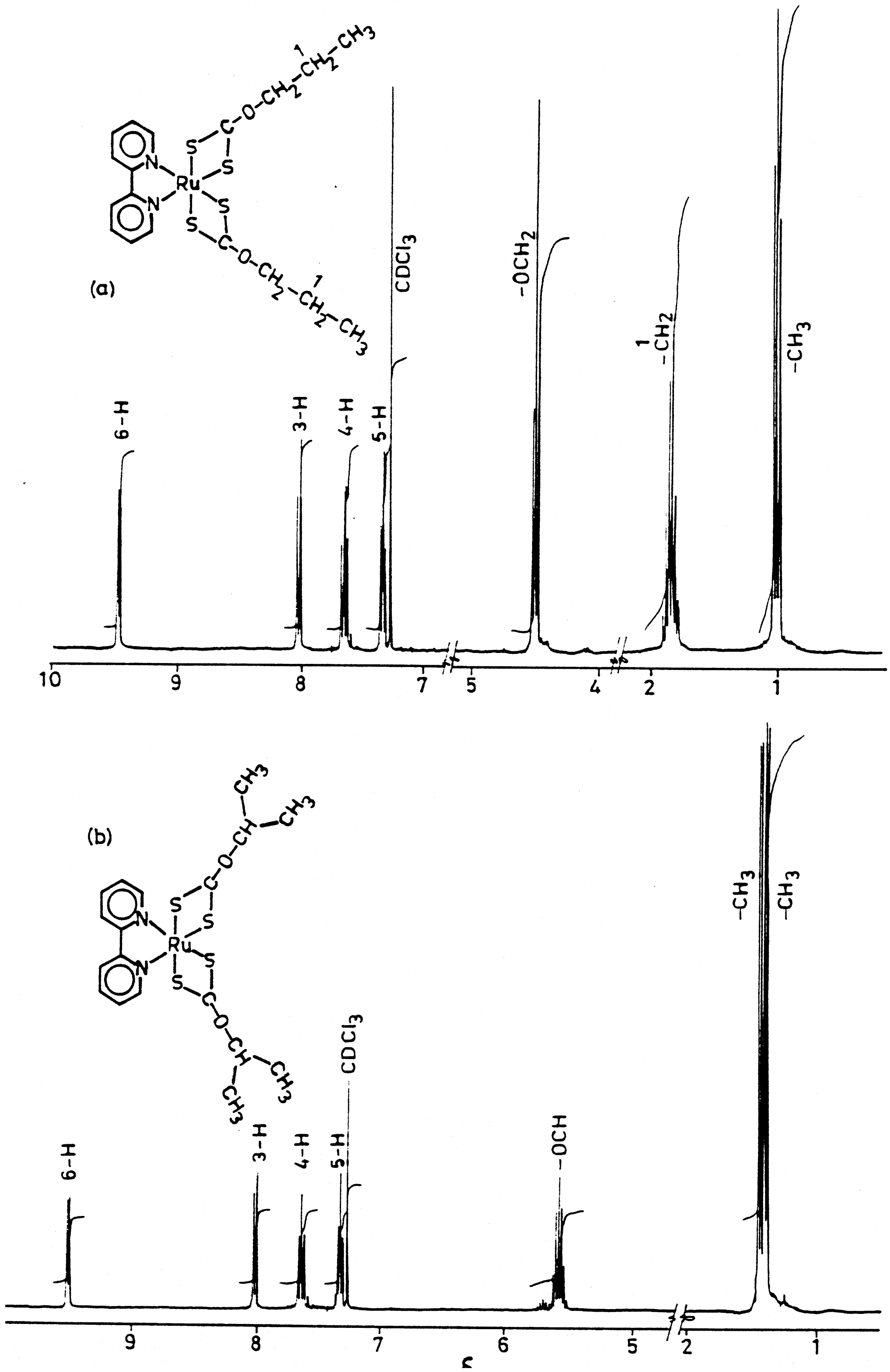

Fig. 1. ^{1}H NMR spectra of (a) [Ru^{II}(bpy)(L^{3})$_2$], **3** and (b) [Ru^{II}(bpy)(L^{4})$_2$], **4** in CDCl$_3$.

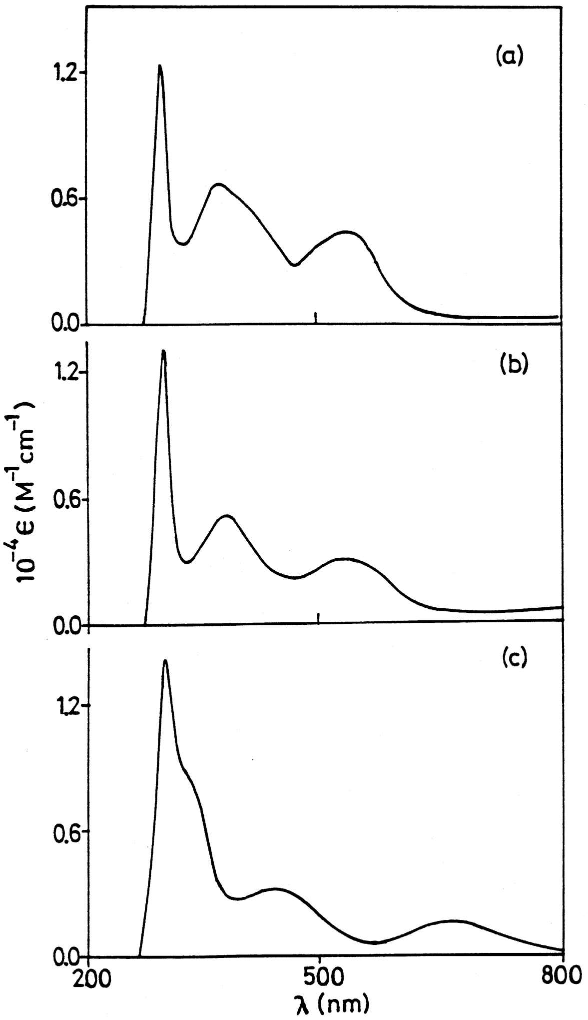

Fig. 2. Electronic spectra of (a) [Ru^{II}(bpy)(L^2)$_2$], **2**, (b) [Ru^{II}(bpy)(L^8)$_2$], **8** and (c) [Ru^{III}(bpy)(L^9)$_2$] ClO_4, **9** in acetonitrile at 298 K.

bpy with dithio ligands, which is in consonance with greater σ-donor and weaker π-acceptor property of L relative to bpy. The electronic spectrum of trivalent ruthenium complex **9** also showing similar three bands but the first two bands are shifted to further lower energy (Table 1). The lowest energy transition at 663 nm is assigned to be the ligand to metal charge-transfer (LMCT) transition as expected for the Ru(III) complexes [38].

Room-temperature emission spectra Emission properties of the complexes (**1**–**8**) were studied in acetonitrile solution at room temperature. The spectral data are listed in Table 1 and the representative spectra are shown in Fig. 3. Excitations of the complexes **1**–**8** near 530 nm (peak position of the lowest energy MLCT band) exhibit very weak emissions, however, excitations near 370 nm (corresponding peak position of the second lowest energy band) result in moderately strong emissions in between 420 to 430 nm (Table 1). The origin of the emissions was further confirmed by the corresponding excitation spectrum of the same solution. It may be noted that the free ligands (KL$^{1-7}$ and NH_4L^8) also showing emissions near 400 nm.

Since both the free ligands (KL$^{1-7}$ and NH_4L^8) and the complexes (**1**–**8**) exhibit emissions around the same positions, the observed emissions for the complexes may therefore be originated from the MLCT band involving primarily the co-ordinated ligands (L).

The lifetime of the excited states of two representative complexes (**2** and **8**) have been determined and are found to be 90 and 95 ns respectively, at room temperature.

Redox properties

All the complexes are electroactive with respect to metal as well as ligand centers. Redox properties of

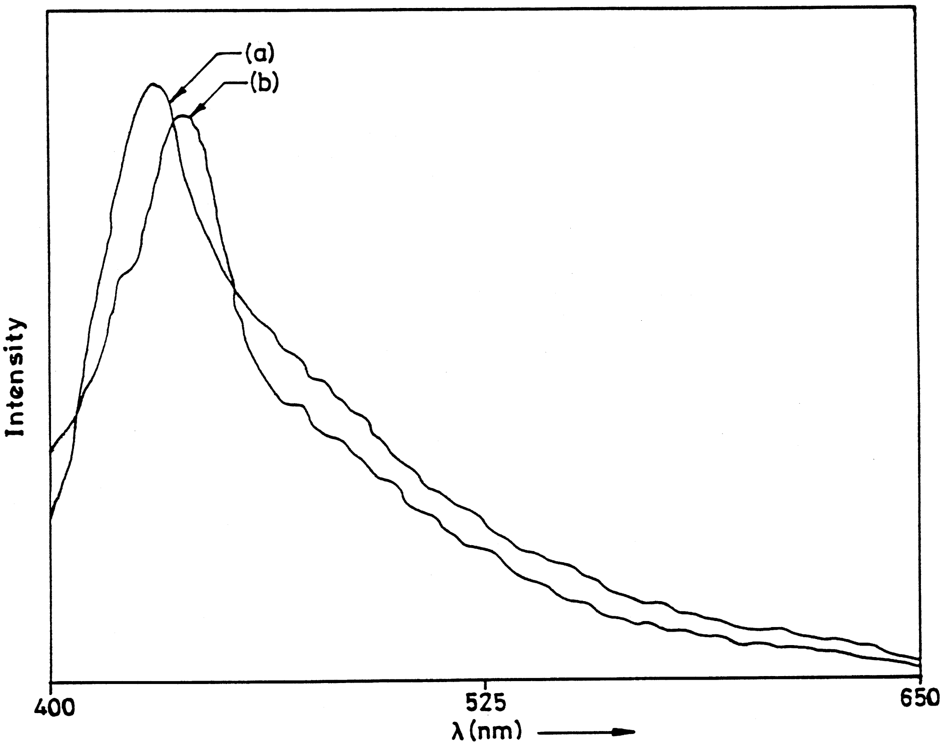

Fig. 3. Emission spectra of (a) $[Ru^{II}(bpy)(L^8)_2]$, **8** and (b) $[Ru^{II}(bpy)(L^7)_2]$, **7** in acetonitrile at 298 K.

the complexes have been studied in acetonitrile solvent by cyclic voltammetry (CV) using a platinum working electrode. The complexes (**1**–**9**) display three redox processes in the potential range ±2.0 V vs Ag/AgCl (tetraethylammonium perchlorate used as an electrolyte, 298 K). Representative voltammograms are shown in Fig. 4. The peak-to-peak separations of the couples lie in the range of 70–90 mV. Reduction potentials data are listed in Table 3.

The ruthenium(III)–ruthenium(II) couple

The complexes **1**–**8** display one reversible oxidation process in the range 0.2–0.4 V and complex **9** exhibits one reversible reduction process at −0.08 V vs Ag/AgCl (Fig. 4) which are assigned to be the ruthenium(III)–ruthenium(II) couple eqn (1) [39].

$$[Ru^{III}(bpy)(L)_2]^+ + e^- \rightleftharpoons [Ru^{II}(bpy)(L)_2] \quad (1)$$

The one-electron nature of the responses is established by current height and constant potential coulometric data. The presence of trivalent ruthenium in the oxidized solutions of **1**–**8** is confirmed by characteristic EPR spectrum of the ruthenium(III) congener (see later). The formal potential of the couple (eqn (1)) varies depending on the nature of ligands L. Although ruthenium ion in the complexes having dithiocarbonate (**1**–**7**) and dithiophosphate (**8**) ligands stabilizes in 2+ oxidation state, the corresponding dithiocarbamate complex (**9**) stabilizes the trivalent ruthenium ion. The low ruthenium(III)–ruthenium(II) potential ($E_{298}{}^0 = -0.08$ V) of complex **9** can account for its stabilization in the trivalent state rather than the bivalent state under atmospheric conditions. Thus the electrochemically as well as chemically generated bivalent congener of **9** is unstable in presence of air, spontaneously oxidized to the trivalent complex **9**. Since the reaction takes place particularly under atmospheric conditions the oxygen in air might be responsible for the stabilization of trivalent ruthenium in the complex **9**.

Under identical experimental conditions, the ruthenium(III)–ruthenium(II) reduction potential of $[Ru(bpy)_3]^{2+}$ appears at 1.27 V [31–35]. Thus substitutions of well known π-acidic bpy ligands from the $[Ru(bpy)_3]^{2+}$ core by two dithio ligands, L in the complexes (**1**–**9**) result in decrease of ruthenium(III)–ruthenium(II) potential by 0.9–1.4 V depending on the nature of ligands L. The monoanionic dithio ligands L^- decrease the overall charge of the complex cation 2+ in $[Ru(bpy)_3]^{2+}$ to zero in the present complexes (**1**–**9**) and that reduction of overall charge provides further electrostatic stabilization of the oxidized trivalent Ru^{III}–L species. This is possibly developed due to the σ-donor character of the dithio ligands [39]. This substantial decrease in Ru^{III}–Ru^{II} potential while moving from $[Ru(bpy)_3]^{2+}$ to $[Ru(bpy)(L)_2]$ (**1**–**8**) and the reversible nature of the voltammograms (Fig. 4)

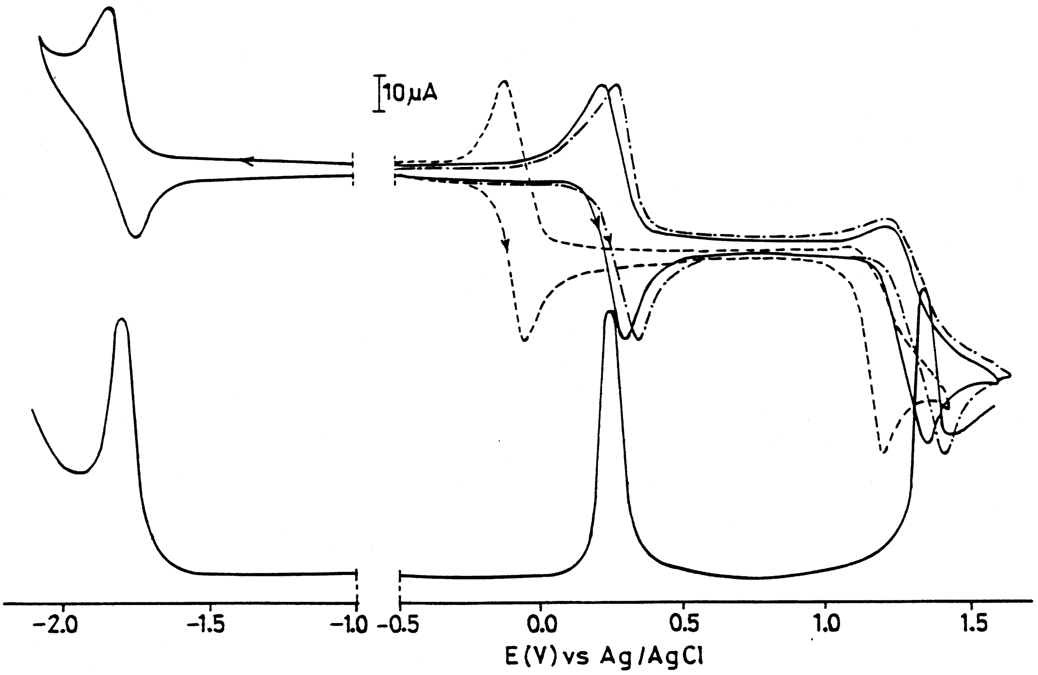

Fig. 4. Cyclic voltammograms of ~10^{-3} M solution of [$Ru^{II}(bpy)(L^2)_2$], **2**, (———), (b) [$Ru^{II}(bpy)(L^8)_2$], **8** (– · –) and (c) [$Ru^{III}(bpy)(L^9)_2$] ClO_4, **9** (- - -) in acetonitrile at 298 K. Differential pulse voltammograms and bipyridine reduction (———) are only shown for complex **2**.

Table 3. Electrochemical data at 298 K[a]

Compound	Ru^{III}–Ru^{II} couple $E_{298}{}^0$ (V) (ΔEp (mV))	n[b]	Ru^{III}–Ru^{IV} $E_{pa}{}^c$ (V)	Ligand reduction $E_{298}{}^0$ (V) (ΔE_p (mV))	ΔE^0 (mV)[d]	ν_{MLCT} (cm^{-1})	
						calc.[e]	obs.[f]
1	0.23 (70)	0.97	1.28	−1.79 (90)	2.02	19291	18832
2	0.25 (80)	0.96	1.34	−1.77 (80)	2.02	19291	18622
3	0.30 (70)	1.05	1.38	−1.73 (80)	2.03	19372	18587
4	0.28 (70)	1.02	1.36	−1.75 (90)	2.03	19372	18519
5	0.34 (80)	1.06	1.42	−1.72 (80)	2.06	19614	18622
6	0.32 (80)	0.95	1.40	−1.72 (80)	2.04	19453	18553
7	0.40 (70)	1.10	1.45	−1.70 (90)	2.10	19936	19084
8	0.30 (80)	1.07	1.40	−1.75 (90)	2.05	19533	18939
9	−0.08 (70)	0.95	1.19	−1.85 (90)	–	–	–

[a] Condition: solvent, acetonitrile; supporting electrolyte, TEAP; reference electrode, Ag/AgCl; solute concentration, ~10^{-3} M; working electrode, platinum wire.

[b] $n = Q/Q'$, where Q' is the calculated Coulomb count for $1e^-$ transfer and Q is the Coulomb count found after exhaustive electrolysis of ~10^{-2} M solution of the complex.

[c] E_{pa} values are considered due to the irreversible nature of the voltammograms.

[d] Calculated by using eqn (4) of text.

[e] Calculated by using eqn (3) of text.

[f] In acetonitrile solution.

indicate the possibility of isolating the trivalent congeners of **1**–**8** under the present mixed-ligand environment.

Although the ruthenium(II)–ruthenium(III) oxidation potentials for the complexes (**1**–**8**) are appreciably low (Table 3), the oxidized trivalent congeners are not stable enough to be isolated (see later).

The complexes (**1**–**9**) exhibit a second irreversible oxidation process in between 1.19–1.45 V vs Ag/AgCl (Fig. 4, Table 3). Although the current height of this irreversible process is higher than the previous one-electron Ru^{III}–Ru^{II} process, the one-electron nature of the second irreversible oxidation process is established with the help of differential pulse voltammetry (Fig. 4). The second one-electron oxidation process could be due to either Ru^{III}–Ru^{IV} oxidation or oxidation of the thiolato group. Since the potential difference (1.10–1.27 V, Table 3) between the two successive processes ($Ru^{II/III}$–second irreversible oxidation process) in the complexes (**1**–**9**) is comparable well with the reported observed potential difference between the two successive redox processes for the ruthenium center ($Ru^{II/III}$–$Ru^{III/IV}$) in mononuclear systems [40, 41], it may therefore be reasonable to assume the second irreversible oxidation as ruthenium(III)–ruthenium(IV) oxidation. However, the possibility of oxidation of the coordinated thiol group cannot be ruled out. The irreversible nature of the process has precluded its further characterization.

Ligand reduction

All the complexes (**1**–**9**) display one reversible reduction in the range $-1.72 \rightarrow -1.85$ V (Table 3, Fig. 4). The one-electron nature of this couple has been established by the current height and differential pulse voltammetry (Fig. 4). Since the free ligands (KL^{1-7}, NH_4L^8, NaL^9) do not exhibit any ligand reduction within the above mentioned potential range, the observed reduction is therefore considered to be reduction of the coordinated bpy ligand. 2,2′-bipyridine is a well known electron-acceptor center and each bpy can accept two electrons in one electrochemically accessible lowest unoccupied molecular orbital (LUMO) [42–45]. Although two successive one-electron bpy reductions are expected for each of the complexes, in practice one reduction corresponding to eqn (2) has been observed within the experimental potential range (-2 V). The other expected reduction could not be detected presumably due to solvent cut-off.

$$\begin{array}{ccc} [\mathrm{Ru(bpy)(L)_2}]^{Z} & +\,e^{-} \rightleftharpoons & [\mathrm{Ru(bpy)(L)_2}]^{Z} \\ z=0,\mathbf{1}\text{–}\mathbf{8};\ z=1,\mathbf{9} & & z=-1,\mathbf{1}\text{–}\mathbf{8};\ z=0,\mathbf{9} \end{array} \qquad (2)$$

Spectroelectrochemical correlation

Complexes **1**–**8** display lowest energy MLCT transitions of the type $t_2(Ru) \rightarrow$ ligand LUMO (where LUMO is dominated by the diimine function of the bpy ligand) in the range 524–540 nm (Table 1). The reversible ruthenium(III)–ruthenium(II) reduction potentials and the ligand (bpy) reductions are appeared in the ranges $0.23 \rightarrow 0.40$ V and $-1.72 \rightarrow -1.79$ V respectively. Here the MLCT transition involves excitation of the electron from the filled $t_{2g}^{\ 6}$ orbital of ruthenium(II) to the lowest π^* orbital of the diimine function. The energy of this band can be predicted from the experimentally observed electrochemical data with the help of eqns (3) and (4) [46, 47].

$$\nu_{\mathrm{MLCT}} = 8065(\Delta E^0) + 3000 \qquad (3)$$

$$\Delta E^0 = E_{298}{}^0(\mathrm{Ru^{III}} - \mathrm{Ru^{II}}) - E_{298}{}^0(\mathrm{L}) \qquad (4)$$

Here $E_{298}{}^0$ (Ru^{III}–Ru^{II}) is the formal potential (in V) of the reversible ruthenium(III)–ruthenium(II) couple, $E_{298}{}^0$ (L) that of the ligand reduction and ν_{MLCT} is the frequency or energy of the charge transfer band in cm^{-1}. The factor 8065 is used to convert the potential difference ΔE from V into cm^{-1} unit and the term 3000 cm^{-1} is of empirical origin. The calculated and experimentally observed ν_{MLCT} transitions are listed in Table 3 and there is a linear relationship between the ν_{MLCT} and ΔE (Fig. 5). Here, the calculated values for all the complexes lie within the 900 cm^{-1} of the experimentally observed charge-transfer energies, which are in good agreement with the previously observed correlation in the other mixed-ligand ruthenium–bipyridine and related systems [48–50].

Electrogeneration of trivalent ruthenium congener and distortion parameters

Chemical oxidations of the complexes (**1**–**8**) in acetonitrile solvent by aqueous ceric ammonium sulphate resulted in green solution initially corresponding to the trivalent congeners of the complexes ($\mathbf{1}^+$–$\mathbf{8}^+$). The oxidized complexes are not stable enough to be isolated in the solid state as it get decomposed to an unidentified product.

Coulometric oxidations of the complexes (**1**–**8**) at a potential 200 mV positive to the corresponding E_{pa} of Ru^{II}/Ru^{III} couple in acetonitrile solution at 298 K generated the same green colored trivalent ruthenium(III) complexes. The observed Coulomb count corresponds to $1e^-$-transfer for all the complexes (Table 3). The resulting oxidized solutions ($\mathbf{1}^+$–$\mathbf{8}^+$) display voltammograms which are superposable on those of the corresponding bivalent complexes (**1**–**8**) which imply that the oxidations here may be stereoretentive in nature. Electrochemically generated oxidized complexes ($\mathbf{1}^+$–$\mathbf{8}^+$) are not stable enough, eventually decomposed to an unidentified product which has precluded their further characterizations. However, in the case of complex $\mathbf{1}^+$ we have been succeeded to record the EPR spectrum by quick freezing the green colored oxidized solution in liquid N_2 (77 K). It exhibits an axial EPR spectrum. The axial nature of the EPR spectrum (Fig. 6) ($g_1 = 2.424$, $g_2 = 2.424$, $g_3 = 1.752$) is characteristic of trivalent ruthenium(III) in axially distorted octahedral environment (low-spin Ru^{III}, $t_{2g}^{\ 5}$, $S = 1/2$) [51, 52].

The green colored isolated trivalent ruthenium(III)–dithiocarbamate complex **9** also exhibits similar axial EPR spectrum (Fig. 6) ($g_1 = 2.405$, $g_2 = 2.405$, $g_3 = 1.756$). The electrochemical reduction of complex **9** at -0.25 V vs Ag/AgCl resulted in a red-brown colored complex corresponding to the bivalent

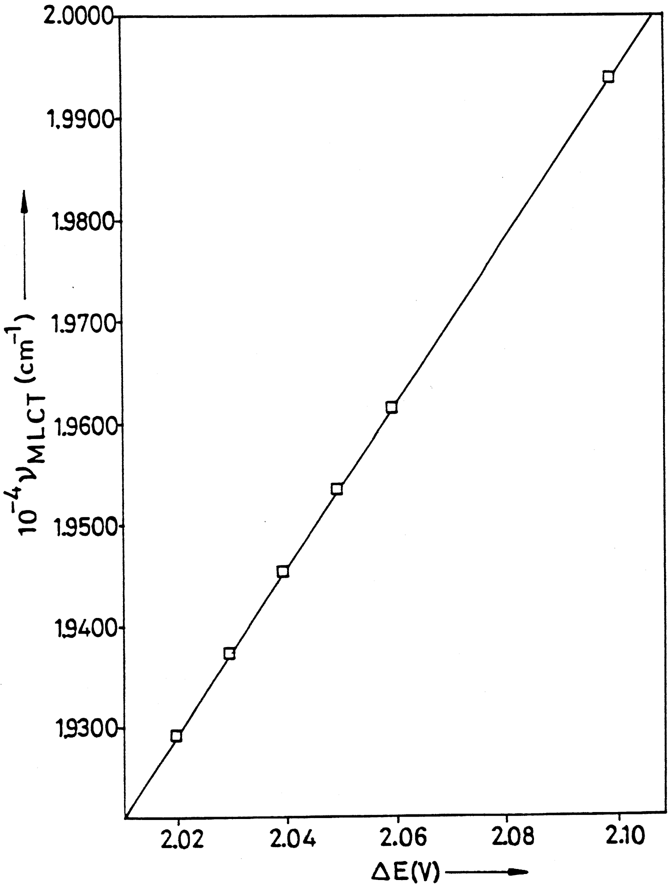

Fig. 5. Least squares plot of the lowest energy metal-to-ligand charge-transfer band (ν_{MLCT}, cm^{-1}) vs the difference in potential (ΔE, V) between Ru$^{II/III}$ couple and the bipyridine reduction.

ruthenium(II) congener (**9**$^-$). The reduced species (**9**$^-$) shows a voltammogram which is superposable on that of the corresponding trivalent complex **9** which indicates the stereoretentive nature of the reduction process. When the same red-brown reduced solution was coulometrically reoxidized at 0.1 V vs Ag/AgCl, the green colored trivalent complex **9** was formed quantitatively. The chemical reduction of **9** by hydrazine hydrate can also generate the bivalent complex **9**$^-$ immediately. The reduced species is unstable under atmospheric conditions, spontaneously oxidizes to trivalent complex **9**.

The theory of EPR spectra of low-spin d^5 complexes are documented in literature [53–57]. The distortion of pseudo octahedral complexes is expressed as the sum of axial (Δ) and rhombic (V) components. The t_2 orbital consists of the components $t_2^0(xy)$, $t_2^+(xz)$, $t_2^-(yz)$. The degeneracy of t_2 orbital is partially removed by axial distortion (Δ), which placed t_2^0 (b) above t_2^+/t_2^- (e). The superimposed (V) then further splits (e) into t_2^+ and t_2^-.

The distortion parameters (Δ and V) and the energies of two optical transitions (ν_1 and ν_2) from ground to upper Kramers doublets can be obtained from the analysis of EPR spectrum using the g tensor theory of low-spin d^5 ions.

The EPR spectrum provides only the absolute g values and so neither their signs nor the correspondence of g_1, g_2 and g_3 to g_x, g_y and g_z are known. There are forty-eight possible combinations based on the labeling (x,y,z) and signs chosen for the experimentally observed g values. For the present case we have chosen the combination $-g_1 = -g_2 > g_3$ (due to axial nature of the spectra g_1 and g_2 are same, Fig. 6) as this particular set gives the orbital reduction factor, $k < 1.0$ The computed values of orbital reduction factor (k), axial distortion (Δ/λ) and the two ligand-field optical transitions (ν_1/λ and ν_2/λ) for the complexes **1**$^+$ and **9** are listed in Table 4. The value of spin–orbit coupling constant (λ) of ruthenium(III) is taken as 1000 cm^{-1} [53–57]. In view of the axial nature of the EPR spectra of the complexes, rhombic distortion (V) is found to be zero.

The low energy near-IR spectrum (maximum wavelength scan up to 2500 nm) of the complex **9** (near-IR spectrum of the complex **1**$^+$ cannot be checked due to its unstable nature) has been checked and it displays one weak transition at 2140 nm (ε, M^{-1} cm^{-1}, 60). In

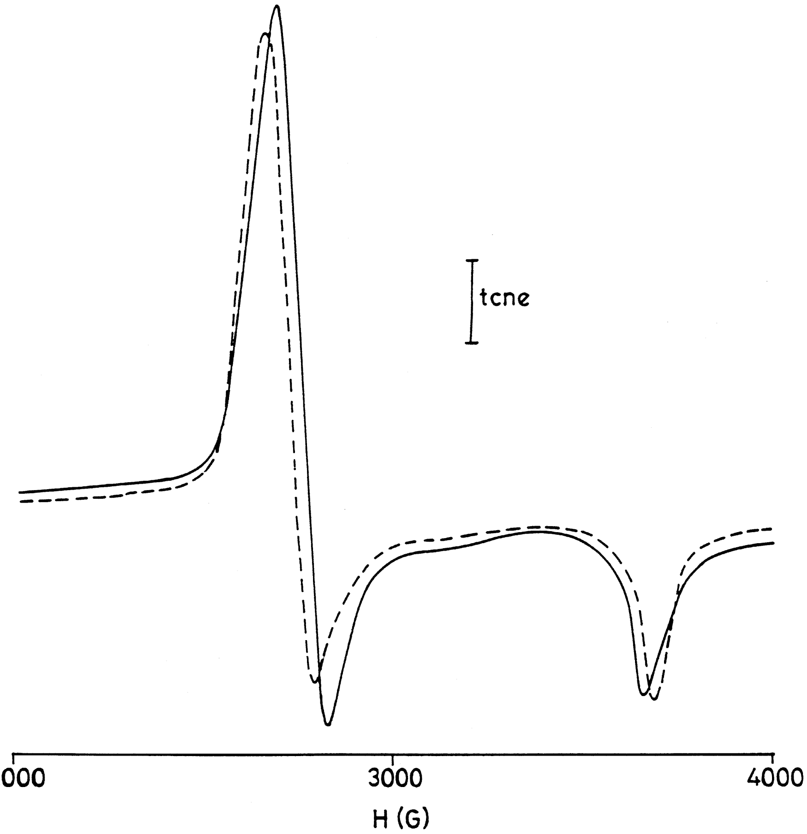

Fig. 6. X-band EPR spectra of coulometrically oxidized complex $[Ru^{III}(bpy)(L^1)_2]^+$, 1^+ (- - -) and $[Ru^{III}(bpy)(L^9)_2]$ ClO_4, **9** (———) in acetonitrile solution at 77 K.

Table 4. The EPR g values[a] and distortion parameters[b]

	Compound	
	1$^+$	**9**
g_1	−2.424	−2.405
g_2	−2.424	−2.405
g_3	1.752	1.756
k	0.889	0.857
Δ/λ	3.689	3.699
V/λ	0.000	0.000
ν_1/λ	3.489	3.497
ν_2/λ	4.339	4.348

[a] In acetonitrile solution at 77 K.
[b] Meanings are given in the text.

view of the involved approximations in the theory, the agreement between the experimentally observed ν_2 and calculated ν_2 value is excellent. Due to instrumental limitation (maximum wavelength scan up to 2500 nm) it has not been possible to compare the ν_1 band.

CONCLUSIONS

We have thus observed that the dithiocarbamate ligand (L^9) along with bipyridine preferentially stabilizes ruthenium(III) in the complex **9**. However, the similar dithiocarbonate (L^{1-7}) and dithiophosphate (L^8) ligands selectively stabilize ruthenium(II) in the complexes **1**–**7** and **8**. Although the reduced ruthenium(II) congener of the complex **9** and the oxidized ruthenium(III) congeners of the complexes **1**–**8** have been observed in the cyclic voltammetric time scale, the reduced and the oxidized species are not stable enough to be isolated using bulk electrolysis as well as by chemical means. The bivalent complexes **1**–**8** exhibit moderately strong emissions at room temperature which are possibly originated from the dithio ligand based MLCT transitions.

EXPERIMENTAL

Materials

Commercially available ruthenium trichloride (S.D. Fine Chemicals, Bombay, India) was converted to

$RuCl_3 \cdot 3H_2O$ by repeated evaporation to dryness with concentrated hydrochloric acid. The [Ru(bpy)Cl_3] was prepared according to the reported procedure [29]. Other chemicals such as 2,2′-bipyridine, diethyl dithio carbamate and solvents were reagent grade and used as received. Silica gel (60–120 mesh) used for the column chromatography was purchased from S.D. Fine Chemicals, Bombay, India. For Spectroscopic and electrochemical studies HPLC grade solvents were used. Commercial tetraethyl ammonium bromide was converted to pure tetraethyl ammonium perchlorate (TEAP) by following an available procedure [58].

Physical measurements

Solution electrical conductivity was checked using a Systronic conductivity bridge, 305. Electronic spectra (900–200 nm) were recorded using a Shimadzu UV 160 spectrophotometer. Near-IR spectrum was recorded by using a Hitachi 330 spectrophotometer. Infrared spectra were taken on a Nicolet spectrophotometer with samples prepared as KBr pallets. Magnetic susceptibility was checked with a PAR vibrating sample magnetometer. ^1H NMR spectra were obtained with the use of 300 MHz Varian FT-NMR Spectrometer. Cyclic voltammetry and coulometric measurements were carried out using a PAR model 273A electrochemistry system. A platinum wire working electrode, a platinum wire auxiliary electrode and an Ag/AgCl reference electrode were used in a three-electrode configuration. TEAP was the supporting electrolyte and the solution concentration was $\sim 10^{-3}$ M. The half wave potential $E_{298}{}^0$ was set equal to 0.5 ($E_{pa} + E_{pc}$), where E_{pa} and E_{pc} are anodic and cathodic cyclic voltammetric peak potentials respectively. The scan rate used was 50 mV s^{-1}. A platinum wire gauze working electrode was used in coulometric experiments. All electrochemical experiments were carried out under dinitrogen atmosphere and are uncorrected for junction potentials. EPR measurements were made with a Varian model 109 E-line X-band spectrometer fitted with a quartz dewar for measurements at 77 K (liquid nitrogen). The spectrum was calibrated by using tetracyanoethylene (tcne) ($g = 2.0023$). The elemental analyses were carried out with a Carlo Erba (Italy) elemental analyzer. Solution emission properties were checked using a SPEX-fluorolog spectrofluorometer.

CAUTION! Perchlorate salts of metal complexes are generally explosive. Care should be taken while handling such complexes.

Treatment of EPR data

An outline of the procedure can be found in our recent publications [38, 59]. We would like to note that a second solution also exists that is different from the chosen one, having small Δ, γ_1 and γ_2 values. The experimentally observed near-IR result clearly eliminates this solution as unacceptable.

Synthesis of ligands and complexes

The ligands KL^{1-7} and NH_4L^8 were prepared by following the reported procedures [60, 61].

The complexes **1**–**7** were synthesized using a general method. Yields varied in the range 80–85%. Specific details are given for one representative case.

(2,2′-*bipyridine*) *bis*(*O-ethyl dithiocarbonate*) *ruthenium*(*II*) [Ru(bpy)$(L^2)_2$] (**2**). Ru(bpy)Cl_3 (100 mg, 0.275 mmol) was dissolved in 20 cm^3 of methanol and stirred for 10 min. To this solution, the ligand KL^2 (132 mg, 0.825 mmol) was added. The initial brown solution of Ru(bpy)Cl_3 immediately turned to red color. The progress of the reaction was monitored periodically by TLC. The solvent was then evaporated under reduced pressure and the crude product was then purified by chromatography on a silica gel (60–120 mesh) column. The pure complex (**2**) was eluted with benzene. On removal of the solvent under reduced pressure fine crystalline complex [Ru(bpy)$(L^2)_2$] was obtained. Yield: 82%.

The complex [Ru(bpy)$(L^8)_2$] (**8**) was prepared by following the above procedure except it requires heating for approximately 30 min after the addition of NH_4L^8 ligand in the starting complex. Yield was 85%.

(2,2′-*bipyridine*) *bis*(*diethyldithiocarbamate*) *ruthenium*(*III*) *perchlorate* [Ru(bpy)$(L^9)_2$]ClO_4 (**9**) Ru(bpy)Cl_3 (100 mg, 0.275 mmol) was dissolved in 20 cm^3 of methanol and stirred for 10 min. To this solution, the ligand NaL^9 (180 mg, 0.825 mmol) was added. The resultant mixture was stirred for 30 min. Initial brown solution of Ru(bpy)Cl_3 was gradually changed to green. The progress of the reaction was monitored periodically by TLC. The crude product was then purified by column chromatography on a silica gel (60–120 mesh) column. The pure complex **9** was eluted with a 4:1 ratio of dichloromethane and acetonitrile solvents. On removal of the solvent mixture under reduced pressure a gummy mass was obtained. It was redissolved in minimum volume of acetonitrile and the concentrated solution was treated with an excess of saturated aqueous $NaClO_4$ solution. The resulting mixture was allowed to stand for 30 min at 273 K. The green colored precipitate thus obtained was collected by filtration and washed thoroughly with ice-cold water. The solid mass was then dried in vacuo over P_4O_{10} Yield: 80%.

Acknowledgements—Financial support received from the Department of Science and Technology, New Delhi, India is gratefully acknowledged. Special acknowledgement is made to the Regional Sophisticated Instrumentation Center, RSIC, IIT Bombay for providing NMR and EPR facilities.

REFERENCES

1. Coe, B. J., Friessen, D. A., Thompson, D. W. and Meyer, T. J., *Inorg. Chem.*, 1996, **35,** 4575.

2. Milkevitch, M., Brauns, E. and Brewer, K. J., *Inorg. Chem.*, 1996, **35,** 1737.
3. Ward, M. D., *Inorg. Chem.*, 1996, **35,** 1712.
4. Rasmussen, S. C., Thompson, D. W., Singh, V. and Petersen, J. D., *Inorg. Chem.*, 1996, **35,** 3449.
5. Cargill Thompson, A. M. W., Jeffery, J. C., Liard, D. J. and Ward, M. D., *J. Chem. Soc. Dalton Trans.*, 1996, 879.
6. Greaney, M. A., Coyle, C. L., Harmer, A. J. and Stiefel, E. I., *Inorg. Chem.*, 1989, **28,** 912.
7. Kroner, R., Heeg, M. J. and Deutsch, E., *Inorg. Chem.*, 1988, **27,** 558.
8. Rao, P. S., Thakur, G. A. and Lahiri, G. K., *Indian J. Chem.*, 1996, **35A,** 946.
9. Santra, B. K., Menon, M., Pal, C. K. and Lahiri, G. K., *J. Chem. Soc. Dalton Trans.*, 1997, 1387.
10. Mukherjee, R. N. and Chakravorty, A., *J. Chem. Soc. Dalton Trans.*, 1983, 2197.
11. Howard, C. A. and Ward, M. D., *Angew. Chem. Int. Ed. Engl.*, 1992, **31,** 1028.
12. Hossain, M., Chattopadhyay, B. K. and Ghosh, S., *Polyhedron*, 1997, **16,** 4313.
13. Sprintschnik, G., Sprintschnik, H. W., Kirsch, P. P. and Whitten, D. G. J., *J. Am. Chem. Soc.*, 1976, **98,** 2337.
14. Gilbert, J. A., Eggleston, D. S., Murphy, W. R. Jr., Gaselowitz, D. A., Gersten, S. W., Hodgson, D. J. and Meyer, T. J., *J. Am. Chem. Soc.*, 1985, **107,** 3855.
15. Gersten, S. W., Samuels, G. J. and Meyer, T. J., *J. Am. Chem. Soc.*, 1982, **104,** 4029.
16. Gilbert, J. A., Geselowitz, D. and Meyer, T., *J. Am. Chem. Soc.*, 1986, **108,** 1493.
17. Honda, K. and Frank, A. J., *J. Chem. Soc. Chem. Commun.*, 1984, 1635.
18. Ellis, C. D., Gilbert, J. A., Murphy, W. R. Jr. and Meyer, T. J., *J. Am. Chem. Soc.*, 1983, **105,** 4842.
19. Vining, W. and Meyer, T. J., *J. Electroanal. Chem. Interfacial Electrochem.*, 1985, **195,** 183.
20. Tanaka, K., Morimoto, M. and Tanaka, T., *Inorg. Chim. Acta*, 1981, **56,** L61.
21. Rillema, D. P., Dressick, W. J. and Meyer, T. J., *J. Chem. Soc. Chem. Commun.*, 1980, 247.
22. Durham, B., Dressick, W. J. and Meyer, T. J., *J. Chem. Soc. Chem. Commun.*, 1979, 381.
23. Dressick, W. J., Meyer, T. J., Durham, B. and Rillema, D. P., *Inorg. Chem.*, 1982, **21,** 345.
24. Gleria, M., Minto, F., Beggiato, G. and Bortolus, P. J., *J. Chem. Soc. Chem. Commun.*, 1978, 285.
25. Durham, B., Caspar, J. V., Nagle, J. K. and Meyer, T. J., *J. Am. Chem. Soc.*, 1982, **104,** 4803.
26. Durham, B., Wilson, S. R., Hodgson, D. J. and Meyer, T. J., *J. Am. Chem. Soc.*, 1980, **102,** 600.
27. Sullivan, B. P., Salmon, D. J. and Meyer, T. J., *Inorg. Chem.*, 1978, **17,** 3334.
28. Casper, J. V. and Meyer, T. J., *Inorg. Chem.*, 1983, **22,** 2444.
29. Anderson, S. and Seddon, K. R., *J. Chem. Res. (S)*, 1979, 74.
30. Pesce, B., *Nuclear Magnetic Resonance in Chemistry*. Academic Press, New York, 1965, p. 174.
31. Ceulemansm, A., Vanquickenborne, L. G., *J. Am. Chem. Soc.*, 1981, **103,** 2238.
32. Root, M. J. and Deutsch, E., *Inorg. Chem.*, 1985, **14,** 1464.
33. Alsfasser, R. and Eldik, R. V., *Inorg. Chem.*, 1996, **35,** 628.
34. Coe, B. J., Meyer, T. J. and White, P. C., *Inorg. Chem.*, 1995, **34,** 593.
35. Juris, A., Balzani, V., Barigelletti, F., Campagna, S., Belser, P., von Zelewsky, *Coord. Chem. Rev.*, 1988, **84,** 85.
36. Lees, A. J., *Chem. Rev.*, 1987, **87,** 711.
37. Brown, G. M., Weaver, T. R., Keene, F. R. and Meyer, T. J., *Inorg. Chem.*, 1976, **15,** 190.
38. Lahiri, G. K., Bhattacharya, S., Ghosh, B. K. and Chakravorty, A., *Inorg. Chem.*, 1987, **26,** 9324.
39. Santra, B. K., Lahiri, G. K., *J. Chem. Soc. Dalton Trans.*, 1997, 129.
40. Bag, N., Lahiri, G. K., Bhattacharya, S., Falvello, L. R. and Chakravorty, A., *Inorg. Chem.*, 1988, **27,** 4396.
41. Lahiri, G. K., Bhattacharya, S., Mukherjee, M., Mukherjee, A. K. and Chakravorty, A., *Inorg. Chem.*, 1987, **26,** 3359.
42. Bhattacharya, S., *Polyhedron*, 1993, **12,** 235.
43. Elliott, C. M., *J. Chem. Soc. Chem. Commun.*, 1980, 261.
44. Tokel-Takvoryan, N. E., Hemingway, R. E. and Bard, A. J., *J. Am. Chem. Soc.*, 1973, **95,** 6583.
45. Morris, D. E., Hanck, K. W. and DeArmond, M. K., *Inorg. Chem.*, 1985, **24,** 977.
46. Goswami, S., Mukherjee, R. N. and Chakravorty, A., *Inorg. Chem.*, 1983, **22,** 2825.
47. Ghosh, B. K. and Chakravorty, A., *Coord. Chem. Rev.*, 1989, **95,** 239.
48. Sullivan, B. P., Caspar, J. V., Johnson, S. R. and Meyer, T. J., *Organometallics*, 1984, **3,** 1241.
49. Dodsworth, E. S. and Lever, A. B. P., *Chem. Phys. Lett.*, 1986, **124,** 152.
50. Greaney, M. A., Coyle, C. L., Harmer, H. A., Jordan, A. and Stiefel, E. I., *Inorg. Chem.*, 1989, **28,** 912.
51. Chattopadhyay, S., Bag, N., Basu, P., Lahiri, G. K. and Chakravorty, A., *J. Chem. Soc. Dalton Trans.*, 1990, 3389.
52. Pramanik, A., Bag, N., Lahiri, G. K. and Chakravorty, A., *J. Chem. Soc. Dalton Trans.*, 1990, 3823.
53. Hill, N. J., *J. Chem. Soc. Faraday Trans.*, 1972, **2,** 427.
54. Bleaney, B. and O'Brien, M. C. M., *Proc. Phys. Soc. London B*, 1956, **69,** 1216.
55. Griffith, J. S., *The Theory of Transition Metal Ions*. Cambridge University Press, London, 1972, p. 364.
56. Daul, C. and Goursot, A., *Inorg. Chem.*, 1985, **24,** 3554.
57. Mahapatra, A. K., Datta, S., Goswami, S., Mukherjee, M., Mukherjee, A. K. and Chakravorty, A., *Inorg. Chem.*, 1986, **25,** 1715.
58. Sawyer, D. T., Sobkowiak, A. and Roberts, J. L., Jr., *Electrochemistry for Chemists*, 2nd edn. Wiley, New York, 1995.
59. Bag, N., Lahiri, G. K. and Chakravorty, A., *J. Chem. Soc. Dalton Trans.*, 1990, 1557.
60. Vogel, A. I., *Text Book of Practical Organic Chemistry*. ELBS, Longman, London, 1978, p. 588.
61. Lefferts, J. L., Mollouy, K. C., Zuckerman, J. J., Haituc, I., Guta, C. and Ruse, D., *Inorg. Chem.*, 1980, **19,** 1662.